Transactions of KSAE, Vol. 33, No. 8, pp.627-635 (August, 2025)

Check for updates

Copyright © 2025 KSAE / 237-06
pISSN 1225-6382 / eISSN 2234-0149
DOI http://dx.doi.org/10.7467/KSAE.2025.33.8.627

〈Technical Paper〉

Novel Control Algorithm of 3 Phase Inverter Using P/Q Vector Prediction Control for EV Power Translation

Eunseok Cho · Sungyong Ha*

Department of Future Vehicle Convergence Engineering, Jungbu University, Gyeonggi 10279, Korea

(Received 26 December 2024 / Revised 31 March 2025 / Accepted 31 March 2025)

Abstract : In response to concerns over carbon emissions and energy shortages, the global automotive industry is prioritizing the development of eco-friendly vehicles. Electric vehicles(EVs), powered solely by electricity, are particularly highlighted as a key solution to these issues. EVs operate with zero emissions by using electric motors and enhance efficiency by recovering energy during braking through regenerative braking technology. This paper proposes a new predictive control technique integrated into the existing inverter system to accurately regulate the power recovered from or produced by the motor. The predictive control method is applied to both the Sector Selection and SPWM methods, accompanied by an analysis of their respective advantages and disadvantages, followed by proposed methods to mitigate the drawbacks. Finally, the performance of the proposed system is validated through simulation.

Key words : EV regeneration, EV efficiency, EV Inverter, EV braking system, Bidirectional power system, Prediction control

Nomenclature

U_L	: motor regeneretive voltage, V
U_S	: inverter output voltage, V
U_{SL}	: voltage between inverter and motor, V
u_L, u_S	: instantanous voltage(motor, inverter), V
i_L	: instantanous inductor current, A
di	: change of current, A
P	: active power
Q	: reactive power
p, q	: instantaneous power(active, reactive)
Ni	: inductor current(next period), A
Np. Nq	: next instantaneous power(active, reactive)
Ci	: inductor current(current period), A

1. Introduction

The global automotive industry is strategically focusing on the development of eco-friendly vehicles as a key global policy, driven by concerns over increasing carbon emissions leading to global warming and the escalating demand for energy, particularly in the transportation sector. Approximately 30 % to 40 % of energy consumption is attributed to transportation, hence the emphasis on developing eco-friendly vehicles that reduce or eliminate the use of fossil fuels.

Eco-friendly vehicles include hybrid electric vehicles (HEVs), electric vehicles(EVs) powered solely by electricity, hydrogen fuel cell electric vehicles (FCEVs), and clean diesel vehicles equipped with emission-reducing technologies. Among these, EVs, which rely solely on electricity and emit zero carbon dioxide, are garnering significant attention as a fundamental solution to environmental and energy scarcity issues.

The powertrain system of electric vehicles(EVs) replaces traditional internal combustion engines with electric motors powered solely by electricity, maximizing fuel efficiency by employing regenerative braking technology. Regenerative braking recovers energy during braking, with braking power proportional to the regenerated energy. Therefore, precise control over both the recovered and output power from the motor is essential for drivers to control vehicle acceleration and braking effectively.

*Corresponding author, E-mail: hsy1396@joongbu.ac.kr

In this paper, a novel predictive control method is applied to the existing inverter system to accurately control the power recovered from or outputted by the motor without the need for a new PID controller. The performance of the proposed system is then validated through simulation.

2. Analysis of Relation Between Inverter Switching and PQ

A typical PWM inverter for electric vehicles can have a total of 6 switching states: 001, 010, 011, 100, 101, and 110. When considering all switches being either fully on (111) or fully off (000), there are a total of 8 possible states. Fig. 1 illustrates the Simplified Inverter for an EV, while Fig. 2 depicts the possible switching states.[1)]

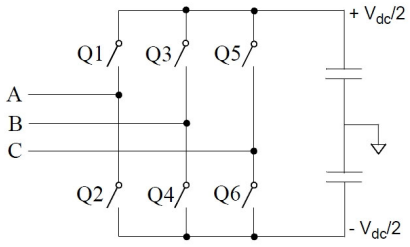

Fig 1. Simplified general schematic of EV inverter

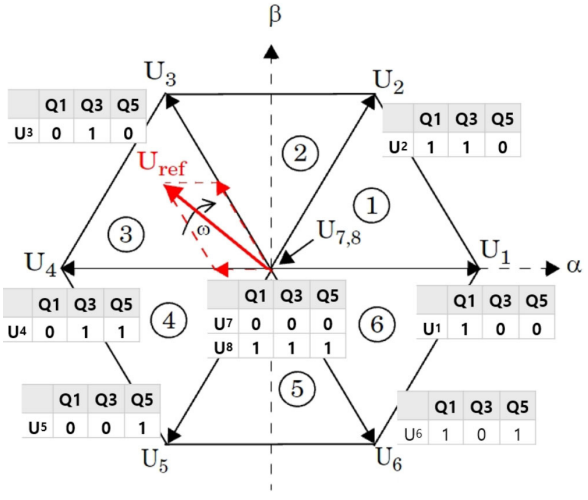

Fig. 2 Switching status of EV inverter

Among the total of 6 switching states, selecting a specific state enables prediction of what P, Q values will be obtained in the next sampling/control cycle through the mentioned steps. Utilizing this information, appropriate switching states can be selected to achieve the desired P, Q values.[1)]

Typically, Q is controlled to be 0, while P is determined based on the motor's output or recovered power. Positive P values indicate motor acceleration, while negative P values denote motor regeneration.[2,3)] This relationship is illustrated in Fig. 3, and its equivalent circuit representation is depicted in Fig. 4.[1)]

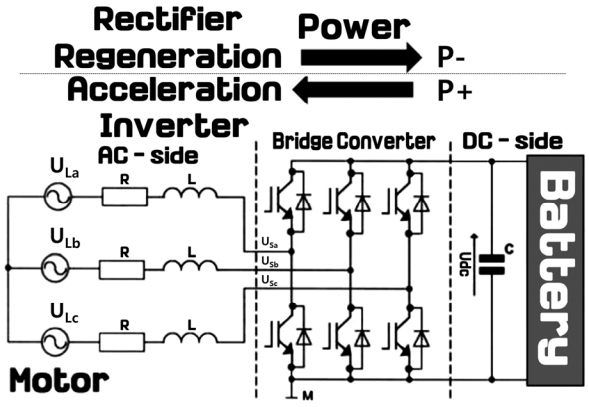

Fig. 3 Acceleration and regeneration of EV power system

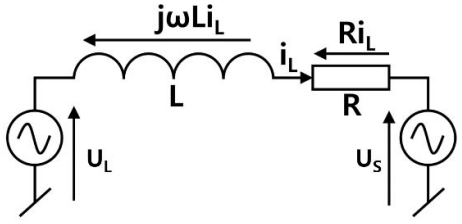

Fig. 4 Equivalent circuit of Fig. 3

When the electrical vector of the inverter rotates on the R, S, T axes and the mechanical vector of the motor rotates, the voltage generated at the motor is denoted as UL, while the voltage at the inverter is denoted as U_S. This is determined based on the switching states described earlier. Once the voltage U_S is determined, the voltage across the inductor, denoted as US_L, is calculated as U_S-U_L. In other words, US_L is determined by U_S.[4)]

When selecting U_S based on the current U_L, U_L is considered a fixed value. This is because, compared to the rate of change of U_L, the sampling/control cycle (20 kHz) is significantly larger, resulting in minimal changes in U_L from the current to the next cycle. This can be expressed by assuming U_L to be 3,600 rpm and represented by Eq. (1)

below.[4)]

$$\Delta T = \frac{1}{20\text{kHz}} = 50us$$

$$60\text{Hz} = 3600\text{rpm}$$

$$360° @60\text{Hz} = 16.667\text{ms}$$

$$1° @60\text{Hz} = 46.2\text{us} \quad (1)$$

$$50\text{us}(20\text{kHz}) = 1.082°$$

$$\Delta u_{L(max)} = \sin(1.082°) - \sin(0°) = 0.018$$

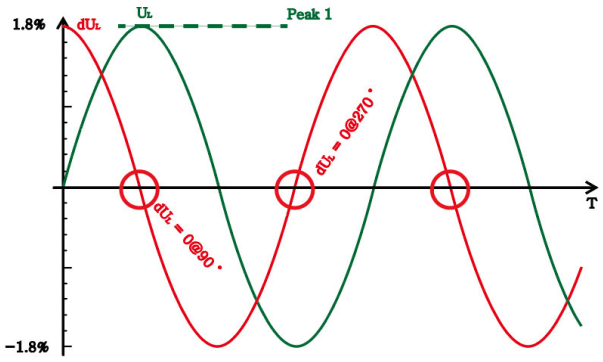

Fig. 5 dU_L wave from when peak U_L is 1

Fig. 5 depicts the rate of change of dUL as UL varies from -1 to 1. According to Eq. (1), it can be confirmed that the change in input voltage until the next cycle is at the level of 1.8 %. This variation depends on the input phase, reaching its maximum at 0° and 180°, while there is no change between the current and next cycle at 90° and 270°.[4)]

2.1 Prediction of Next Cycle Current through Fixed Input Voltage and Assumed Current

It was previously stated that the magnitude and phase of the motor voltage are relatively stable until the next cycle, thus they are assumed to be fixed for interpretation. Additionally, for geometric interpretation/explanation of inductor current, specific values are assumed for magnitude and phase. However, during actual system application (Simulation), values detected by current sensors are utilized.[5-8)]

Predicting the next cycle current based on fixed input voltage and assumed current follows the calculation process outlined below and is represented in Fig. 6.

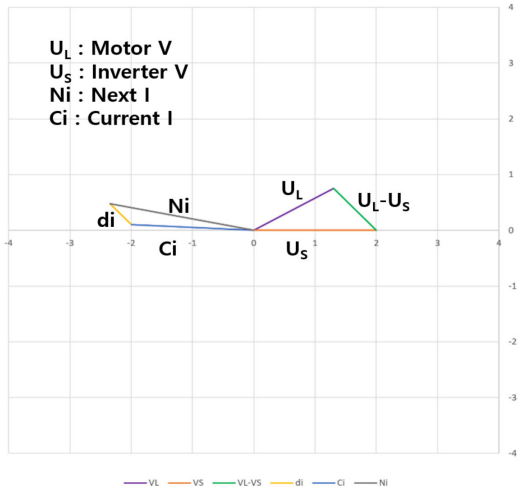

Fig. 6 Predict current (Ni) in the next cycle

① The α and β components of the motor regenerative voltage u_L are obtained.

$$u_{L\alpha} = U_L \cos(\theta), u_{L\beta} = U_L \sin(\theta)$$

② The α and β components of the selected inverter voltage (u_S) are obtained in the same manner as in ① above.

③ α, β of di of inductor are obtained through $u_{L\alpha}$, $u_{L\beta}$, $u_{S\alpha}$, $u_{S\beta}$

$$di_\alpha = \frac{u_{L\alpha} - u_{S\alpha}}{L} dt, \qquad di_\beta = \frac{u_{L\beta} - u_{S\beta}}{L} dt$$

④ The α and β components of the assumed inductor current are obtained in the same way as in ①

⑤ The α and β components of the assumed current are added to the α and β components of di, respectively, to obtain i_α and i_β in the next cycle (next cycle current prediction).

2.2 p and q Control by Predicting the p and q Values of the Next Cycle

$$\text{Np} = u_{L\alpha} i_\alpha + u_{L\beta} i_\beta$$
$$\text{Nq} = u_{L\beta} i_\alpha - u_{L\alpha} i_\beta \quad (2)$$

Fig. 7 shows the trajectory of the current changes when Sector 1 is selected, while Fig. 8 illustrates the scenarios when Sectors 1 through 6 are chosen. Fig. 9 depicts the trajectory of the predicted p and q values for the next cycle when Sector 1 is selected, and Fig. 10 shows the scenarios for Sectors 1 through 6.

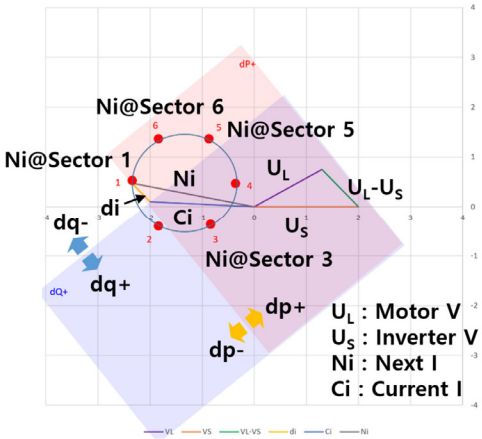

Fig. 7 Changes of predicted next current according to sector change

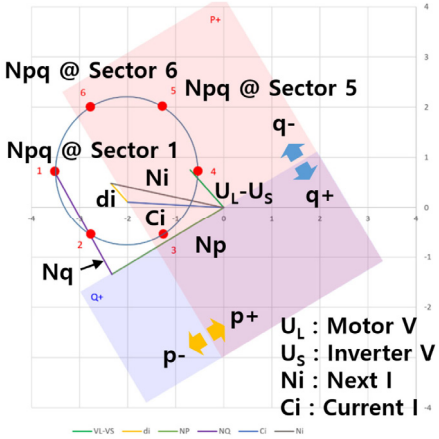

Fig. 9 Change of P and Q according to sector change

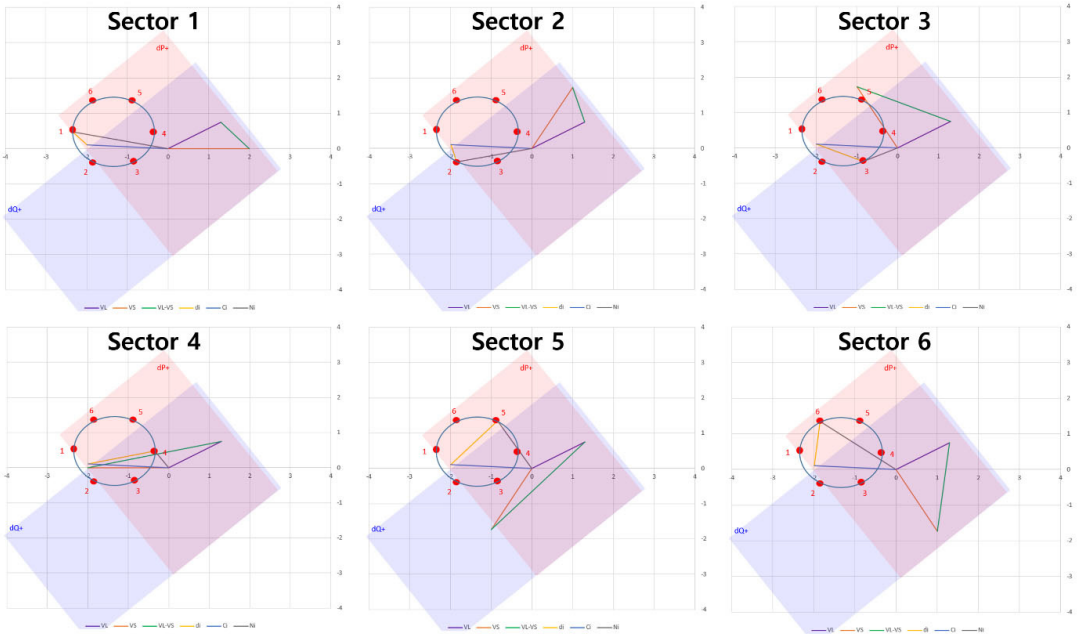

Fig. 8 Predict current (Ni) in the next cycle @Sector 1~6

2.3 P/Q Control Simulation (Sector Selection)

Now, we are able to determine the P and Q for the next cycle. As mentioned earlier, by predicting the values of p and q according to the change in sectors and continuously selecting the sector closest to the reference P and Q values through Distance Calculation, we can effectively control p and q. This method allows for efficient control without the need for additional controllers like PID. Distance Calculation uses a standard formula, as shown in Eq. (3), to calculate the distance between two points. From the calculated distances of p and q for each sector, we select the sector with the p and q values closest to the reference P and Q. Although the block diagram may appear more complex compared to a typical PID algorithm, this simple comparison algorithm is much more advantageous in terms of computation.

$$\text{Distance} = \sqrt{P^2 + Q^2} \tag{3}$$

Fig. 11 depicts the block diagram of the algorithm, while Fig. 12 shows the waveform of controlling P to 30 and Q to

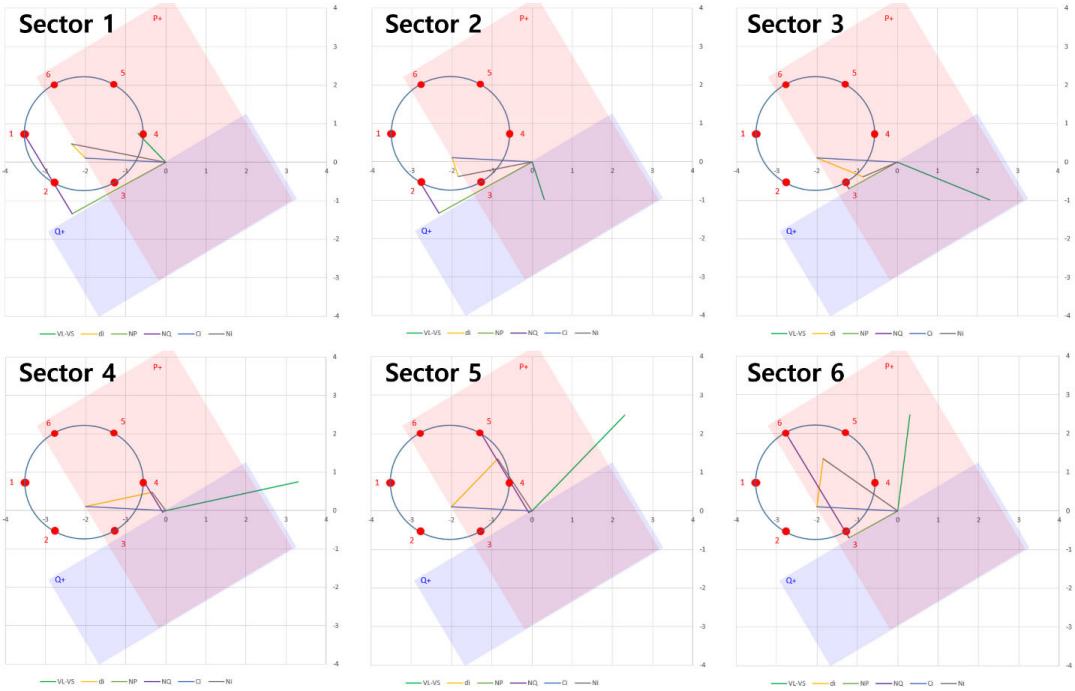

Fig. 10 Change of P and Q according to sector change(Sector 1~6)

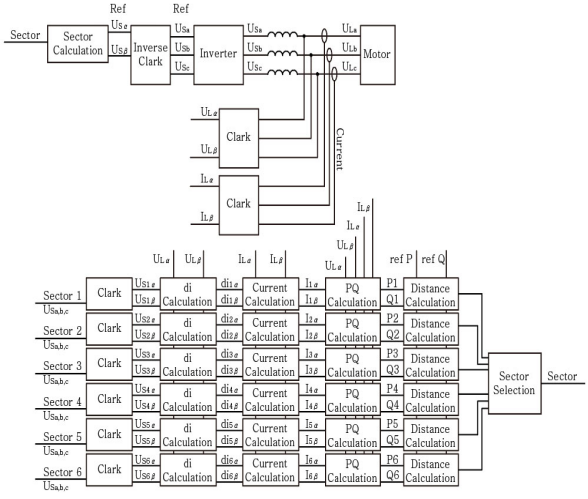

Fig. 11 Block diagram of predictive PQ control

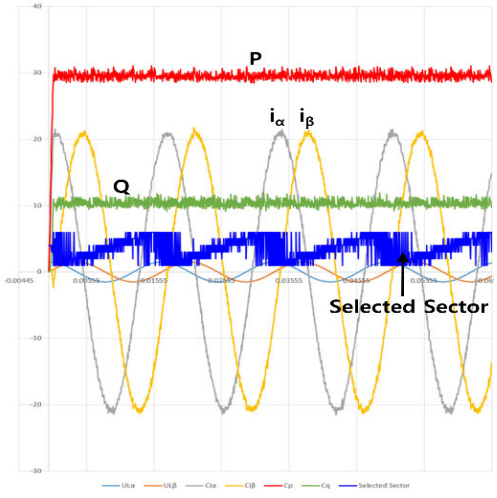

Fig. 12 P/Control simulation (Sector selection)

10 using the predictive method for the next cycle without a controller. Typically, Q is controlled to 0, but it was controlled to 10 to demonstrate the characteristics of the proposed algorithm.

The switching frequency is not determined by the control cycle of the MCU, but rather by how quickly a sector is selected and changed. Therefore, it can be confirmed through actual operation or simulation. In this system, it was measured at 7.26 kHz.

2.4 P/Q Control (Vector Calculation)

While the previous section described the most efficient method for selecting sectors to control p and q to the desired values, this section proposes a method to directly calculate

vectors that satisfy the desired p and q instead of selecting sectors. Once the vectors are obtained, they can be implemented using SPWM(Sinusoidal Pulse Width Modulation).

① The α and β components of the motor regenerative voltage u_L are obtained.

$$u_{L\alpha} = U_L \cos(\theta), u_{L\beta} = U_L \sin(\theta)$$

② Obtain the α and β components of the current required to achieve the q and p command values.

$$p = u_{L\alpha} i_\alpha + u_{L\beta} i_\beta$$

$$q = u_{L\beta} i_\alpha - u_{L\alpha} i_\beta$$

$$i_\alpha = \frac{u_\alpha p + u_\beta q}{u_\alpha^2 + u_\beta^2}$$

$$i_\beta = \frac{u_\beta p - u_\alpha q}{u_\alpha^2 + u_\beta^2}$$

③ Find the difference between the current obtained in (2) and the present current to obtain the necessary α and β components of di.

④ By using the α and β components of di, the α and β components of the inverter voltage U_S are obtained.

$$u_{S\alpha} = u_{L\alpha} - L\frac{di_\alpha}{dt}$$

$$u_{S\beta} = u_{L\beta} - L\frac{di_\beta}{dt}$$

As shown in Fig. 13, the simulation results are shown in Fig. 14. Simulation conditions were set at switching frequency 20 kHz, P = 30, and Q = 10.

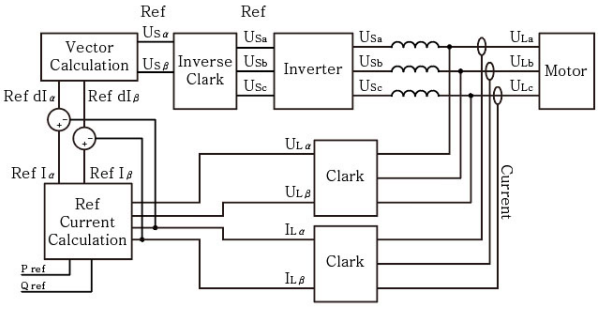

Fig. 13 p and q control block diagram implemented by p and q prediction method

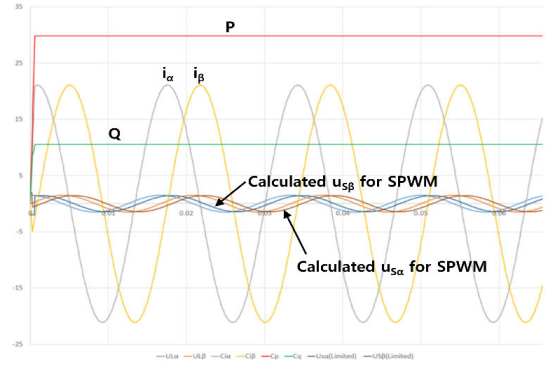

Fig. 14 p, q control simulation implemented by P and Q prediction method

2.5 Comparison of Sector Selection and SPWM

When controlling with a switching and control frequency of 20 kHz and setting P to 30 and Q to 10, both sector selection and Sinusoidal Pulse Width Modulation (SPWM) methods exhibit the characteristics/features shown in Fig. 15 below.

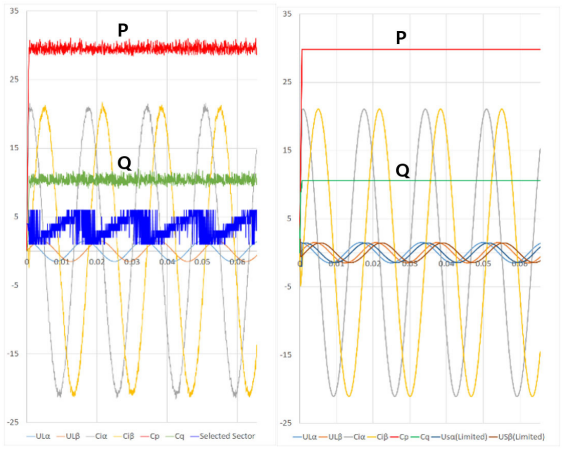

Fig. 15 Sector selection (Left), sinusoidal vector calculation/ SPWM (Right)

2.6 Comparison of Inductor Current(Sector Selection and SPWM)

Figs. 16~19 show comparison of 2 types of control algorithm suggested above. As you can see in Fig. 17 and Fig. 19, the PQ control algorithm using sector selection method has higher harmonic distortion than SPWM method.

2.7 Steady State Output Offset Error

Due to the assumption that the input voltage is almost constant in the control period (50us at 20kHz switching), a

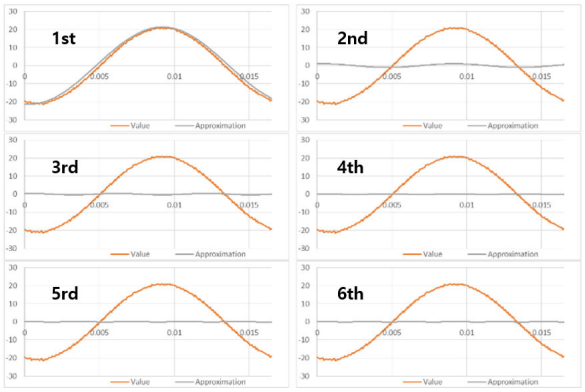

Fig. 16 Harmonic wave forms(Sector selection)

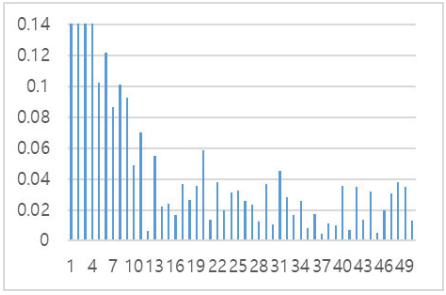

Fig. 17 Harmonic size according to order(Sector selection)

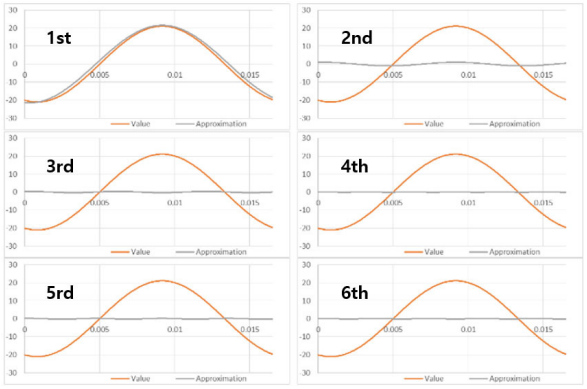

Fig. 18 Harmonic wave forms(SPWM)

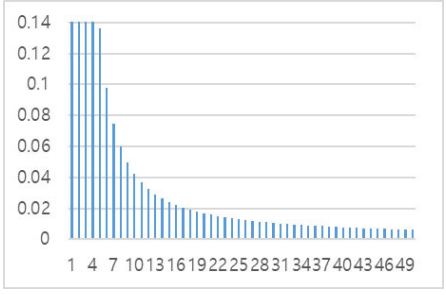

Fig. 19 Harmonic size according to order(SPWM)

small steady-state error occurs(Table 1). It can be simply improved by adding calculated offset value because the error is not a continuously changing value as following block diagram and simulation result(Fig. 20, Fig. 21).

Table 1 Comparison of Sector Selection Method and Sinusoidal Vector Calculation (SPWM) Method (THD : Total Harmonic Distortion)

Item	Sector Selection	SPWM
Controlled p	29.55	29.81
Controlled q	10.38	10.56
Ripple p	2.62	0
Ripple q	2.82	0
Error p	0.446	0.194
Error q	-0.384	-0.564
Switching frequency	7.26 kHz	20 kHz
Switching loss	Low (Good)	High (Bad)
THD (Input Current)	5.54 %	5.53 %
THD (Output Voltage)	High (Good)	Low (Best)

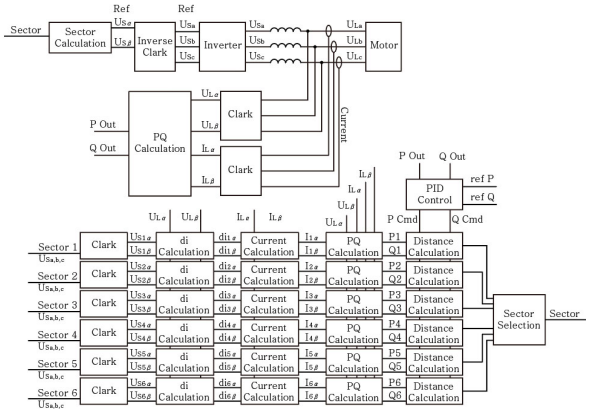

Fig. 20 System block diagram(Offset algorithm)

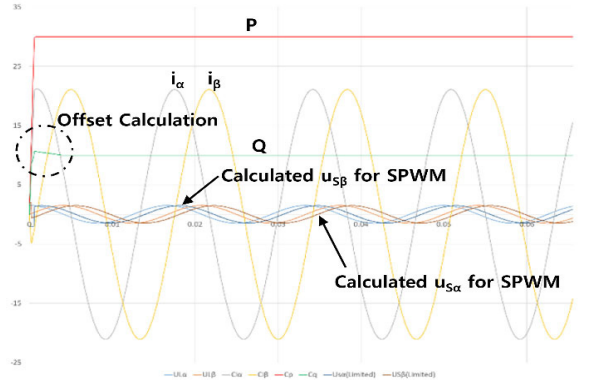

Fig. 21 Simulation result(Offset algorithm)

2.8 PID Control for Offset Error

As depicted in Figs. 22~25 below, a simple PID controller can be added instead of the Offset Controller.

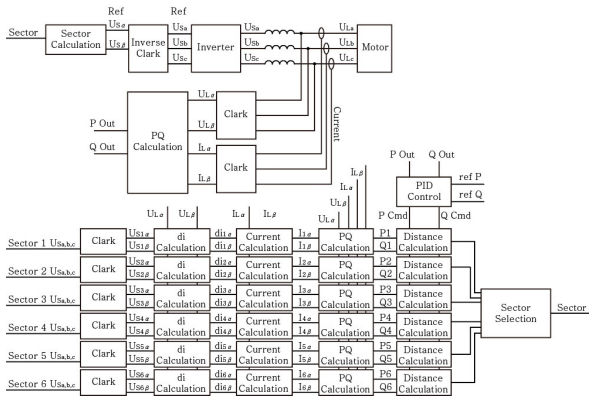

Fig. 22 System block diagram with PID controller(Sector selection)

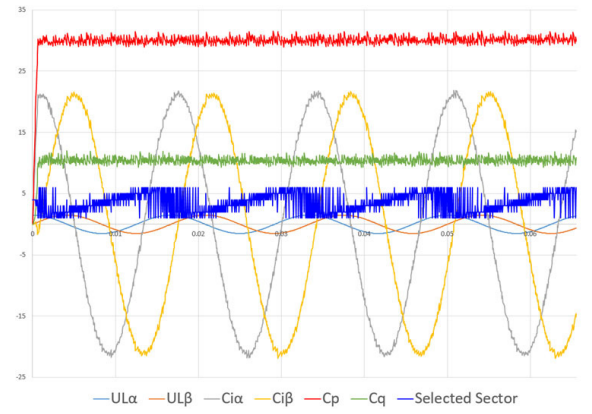

Fig. 23 Simulation result(Sector selection, PID)

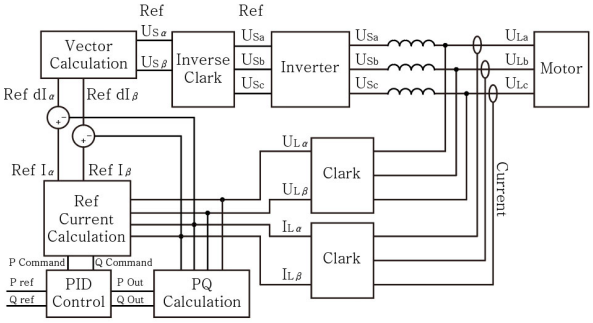

Fig. 24 System block diagram with PID controller(SPWM)

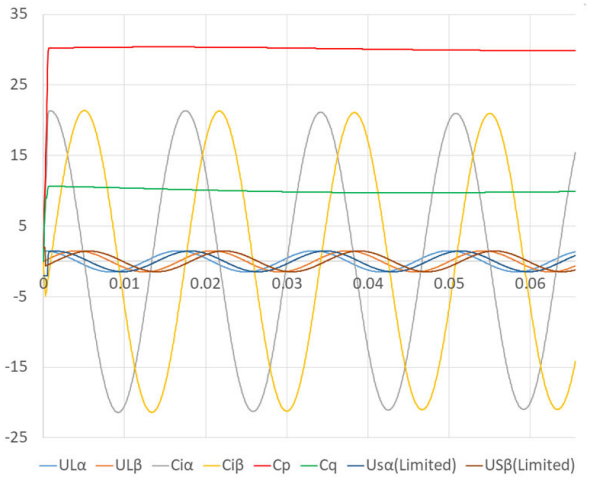

Fig. 25 Simulation result(SPWM, PID)

3. Conclusion

This paper proposes a novel predictive control technique applicable to inverter control in electric vehicles. The proposed control method aims to accurately regulate the power recovered from or supplied to the motor by integrating with existing inverter systems. The predictive control technique is applied to both the Sector Selection method and Sinusoidal Pulse Width Modulation(SPWM) method, analyzing their respective advantages and disadvantages and proposing methods to address the drawbacks. Additionally, an Offset algorithm is employed to eliminate steady-state errors inherent in the proposed system's structure. Finally, the performance of the proposed system is validated through simulation, assessing how well it tracks the demanded P and Q values. However, future research should include a dynamic analysis to evaluate how well P and Q track with variations in motor rotational speed.

Acknowledgements

This study was carried out with the support of the KOREA Ministry of Land, National Transport Science and Technology Agency Promotion (RS-2023-00253588) and Joongbu University Research & Development Fund, in 2025.

References

1) E. S. Cho, "EV Control Technology Using Prediction Controller Suitable for Regenerative Braking and PLL with Excellent Dynamic Characteristics and

Protection," Ph. D. Dissertation, Joongbu University, Goyang, 2025.
2) E. S. Cho and S. Y. Ha, "PLL Technique of Regenerative Braking System Capable of Responding to Immediate Input Change," Transactions of KSAE, Vol.32, No.6, pp.529–534, 2024.
3) E. S. Cho and S. Y. Ha, "The Research of Effective PWM Noise Reduction Methods for EV PTC Heater," Transactions of KSAE, Vol.32, No.9, pp.695–702, 2024.
4) M. H. Rashid, Power Electronics Handbook, p.427, 2001.
5) M. C. Shin, E. S. Cho, J. M. Jung and Y. K. Lee, "3kW Isolated DC-DC Converter Design Method with High Step-Down Ratio and Efficiency for Electronic/Hybrid Car," Korea Science & Art Forum, pp.435–442, 2015.
6) E. S. Cho, J. S. Ko and Y. K. Lee, "The Research of Bi-Directional Step-Up Down Simple H Bridges Inverter for Green Car or Light System," The Korean Society of Science & Art, pp.689–695, Dec 2014.
7) J. K. Kim, E. S. Cho, Y. K. Lee, J. W. Lee and J. H. Lee, "C++ Based Dynamic Model of AC Induction Motor in Discrete Time Domain," ITEC Asia-Pacific, pp.272-276, 2016.
8) Y. K. Lee, J. K. Kim and E. S. Cho, "Design of Bus Side RCD Snubber Circuit for Three-Phase High Power Inverters," Canadian Journal of Electrical and Computer Engineering, Vol.41, No.1, pp.55–61, 2018.